Multifunctional Composites

Mater. Res. Soc. Symp. Proc. Vol. 1718 © 2015 Materials Research Society
DOI: 10.1557/opl.2015.35

Thermal, Mechanical and Magneto-Mechanical Characterization of Liquid Crystalline Elastomers Loaded with Iron Oxide Nanoparticles

Stephany Herrera-Posada[1], Barbara O. Calcagno[2], and Aldo Acevedo[1]
[1]Department of Chemical Engineering, University of Puerto Rico, Mayagüez 00681, Puerto Rico
[2]Department of General Engineering, University of Puerto Rico, Mayagüez 00681, Puerto Rico

ABSTRACT

Liquid crystalline elastomers (LCEs) are materials that reveal unusual mechanical, optical and thermal properties due to their molecular orientability characteristic of low molar mass liquid crystals while maintaining the mechanical elasticity distinctive of rubbers. As such, they are considered smart shape-changing responsive systems. In this work, we report on the preparation of magnetic sensitized nematic LCEs using iron oxide nanoparticles with loadings of up to 0.7 wt%. The resultant thermal and mechanical properties were characterized by differential scanning calorimetry, expansion/contraction experiments and extensional tests. The magnetic actuation ability was also evaluated for the neat elastomer and the composite with 0.5 wt% magnetic content, finding reversible contractions of up to 23% with the application of alternating magnetic fields (AMFs) of up to 48 kA/m at 300 kHz. Thus, we were able to demonstrate that the inclusion of magnetic nanoparticles yields LCEs with adjustable properties that can be tailored by changing the amount of particles embedded in the elastomeric matrix, which can be suitable for applications in actuation, sensing, or as smart substrates.

INTRODUCTION

Coupling the molecular orientability characteristic of low molar mass liquid crystals with the mechanical elasticity of slightly crosslinked polymeric networks gives rise to a group of functional responsive materials known as liquid crystalline elastomers (LCEs). When external stimuli are applied, such as temperature, the constituent anisotropic molecules with mesomorphic features, known as mesogens, can undergo reorientations causing deformations of the polymeric chains to which these molecules are attached and in consequence fluctuations in its physical properties. Among these fluctuations are the dramatic reversible length changes of uniformly oriented LCEs and the variations of optical properties (i.e.birefringence) when transitions from disordered to ordered states, or vice versa, are occurring. Inversely, by the application of mechanical strains or deformations, it is possible to induce reorientation of the mesogens which is manifested in alterations of mechanical and optical properties as well [1, 2]. Therefore, LCEs are ideal candidates for applications in actuation, sensing and smart substrates, amongst others [3].

Incorporation of inorganic fillers with special features such as sensitivity to external fields or light irradiation, can produce more efficient materials. Reports on the addition of carbon nanotubes to LCEs have shown to expand the number of stimuli that can be used to trigger shape changes, such as light irradiation at different wavelengths or application of electric fields [4-6]. The introduction of magnetic particles into LCEs has limited precedents [7-9] and in this regard, iron oxide nanoparticles are proposed in order to produce magnetic responsive elastomers that

can be stimulated remotely. Nevertheless, introduction of particles into a liquid crystal matrix can negatively affect their internal structure. In this report, the systematic evaluation of the effect of particle content on the thermal, thermo-mechanical, mechanical and magneto-mechanical properties of magneto-sensitized LCEs using oleic acid-coated iron oxide nanoparticles is presented. Understanding the effect of particle concentration on the structure and performance properties of the LCEs is necessary to optimize formulation parameters for specific applications. For example, applications in bioengineering would require low particle content to decrease potential risks associated with particle leaching and operating temperature (or LC phase range) below 40 °C to prevent cell death.

EXPERIMENTAL DETAILS

Liquid crystalline elastomers synthesis

Liquid crystalline elastomer films were prepared following the two steps crosslinking reaction proposed by Finkelmann [10], using 10% of crosslinker, 1,4-(10-undecenyloxy) benzene, 11UB, synthesized according to reported methods [11] and 80% of mesogenic monomer, 4-(3-butylenoxy)benzoic acid methyl ester, MBB, purchased from TCI America. The polymer backbone, poly(methylhydrosiloxane, (PHMS Mn 1700-3200, Sigma-Aldrich, USA) was simultaneously mixed with the mesogenic monomer and the crosslinker followed by 1 mL of the reaction solvent (toluene, HPLC grade, Sigma-Aldrich, USA), and 20 to 50 μL of a 1 wt% Pt catalyst (1,5-cyclooctadienyl platinum(II) dichloride, Sigma-Aldrich, USA) solution prepared in dichloromethane (Sigma-Aldrich, USA, used as received). The mixture was transferred to a sealed PTFE (Teflon™) mold and left to react at 65 °C for 1 h. The resultant gel-like material was then removed from the mold and subjected to a constant load, while the crosslinking reaction was still occurring. After an alignment was observed (optical transparency) the films were left standing at 40 °C for 48 h to ensure completion of the reaction. Finally the films were rinsed with toluene in order to remove any unreacted material. In order to prepare the magnetic LCEs, different solutions of oleic acid-coated iron oxide nanoparticles (d_H = 20 nm, Sigma-Aldrich, USA) in toluene were used as the reaction solvent. Particle concentrations of 0.07, 0.17 and 0.25 wt/v% were used to give approximately 0.2, 0.5 and 0.7 wt% of particles in the LCE matrix, respectively.

Materials characterization

Thermal transitions were measured on a TA Instruments Q2000 DSC under a nitrogen flow of 50 mL/min in heating-cooling-heating cycles at rates of 10°C/min. The reported values for the glass transition correspond to the midpoint of the step change, while the nematic-to-isotropic transition was identified as the maximum of the endothermic peak in the second heating heat flow trace. In order to quantify the mechanical elasticity or the stiffness, tensile tests were performed parallel and perpendicular to the director (stretching direction) using a stress-controlled rheometer Anton Paar MCR 302 equipped with an extensional test fixture (X-pansion Instruments SER2), and with a convection oven (CTD 450). The strain rate was constant at 0.02 s^{-1} and the temperature was set such as $T_{test} = 0.7\ T_{ni}$ to obtain a similar nematic state. Thermo-mechanical (expansion/contraction) experiments were conducted by manually recording the film length at 5 °C steps from 90 to 20 °C. The temperature was held fixed until stabilized in an INSTEC HSC302-mK1000A thermal stage and was independently verified with a surface thermocouple connected to the aluminum stage. Magneto-mechanical experiments were

performed with an induction heater apparatus Ambrell EASYHEAT LI (RHS). The samples (about 2.6 cm in length) were placed vertically in the middle of the coil (four turns, 3.16 cm ID, 2.97 cm height) clamped at one end and suspended at the other. The change in position of the suspended end was monitored by taking pictures with a camera every 20 seconds, and the data was collected using ImageJ software. Several on/off cycles, of 8 min each, were run at a constant oscillation frequency of 298 kHz and a field strength of about 49 kA/m.

RESULTS AND DISCUSSION

Figure 1 shows the variation of the glass transition and nematic-to-isotropic phase transition temperatures of the elastomers as a function of magnetic content. Unlike other liquid crystalline elastomer composite systems, where the addition of external fillers have little effect on the thermal transitions [9,12], it is observed a reduction from 63.3 ± 0.6 to 34.3 ± 0.8 °C for the nematic-to-isotropic transition temperature and from -4.5 ± 1.2 to -17.7 ± 1.2 °C for the glass transition upon increasing particle loading up to 0.7 wt%. The effect of the nanoparticles in the T_g is probably due to repulsive or poor interactions between the particles surface and the polymer matrix [13, 14]. On the other hand, the drop in the nematic-to-isotropic transition could be attributed to the particles acting as impurities, reducing therefore the liquid crystalline order of the material [15].

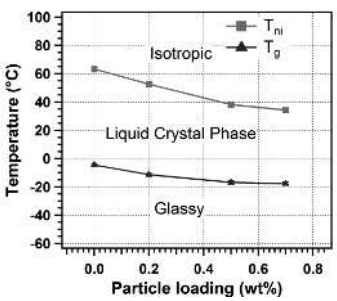

Figure 1. Phase diagram of the LCEs loaded with oleic acid-coated iron oxide nanoparticles.

The reversible thermal actuation ability of the elastomers is depicted in Figure 2. It is observed that the deformation (expansion upon cooling/contraction upon heating) is also particle-loading dependent, with a reduction of the relative sample length λ/λ_0 at the lowest temperature studied, from 1.52 ± 0.03 for the neat LCE to 1.29 ± 0.03 for the highest concentration. This can be attributed to a more restricted movement of the mesogenic molecules and in consequence to the polymeric chains due to particles occupying free volume within the elastomeric matrix. It can also be related to the elasticity of the resultant composite material, and how difficult is to deform a system with particles that can act as mechanical reinforcement. It is known that for many isotropic polymer composites, the stiffness of the polymeric matrix is enhanced by adding inorganic particles which are generally stiffer than the matrix [16]. Figure 3 shows this reinforcement on the LCEs mechanical properties which are in this case anisotropic. The Young's moduli measured at a same T_{test} within the mesophase range, for both directions parallel and perpendicular to the principal orientation axis (director), increases once

nanoparticles are added and this has been reported for some carbon nanotubes LCE composites in the parallel direction [4, 6]. From Figure 2 it can also be noticed that there is no hysteresis between cooling and heating cycles, indicating that the particles are not affecting the reversible deformation distinctive of LCEs.

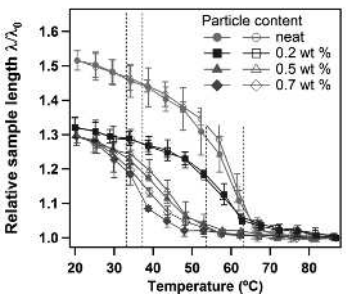

Figure 2. Relative sample length, λ/λ_0, of the elastomers as a function of particle loading during cooling (closed symbols) and heating (open symbols). [λ_0 is the film length at the isotropic phase. Dashed lines correspond to the values of T_{ni}].

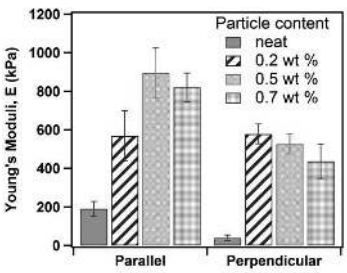

Figure 3. Young's moduli of the elastomers measured parallel and perpendicular to the stretching direction, as a function of particle loading.

The magneto-induced actuation for a 0.5 wt% nanoparticle loaded LCE is shown in Figure 4a. The magnetic LCE can experience reversible contraction/expansions when subjected to on/off alternating magnetic field cycles and its behavior persist at least for the observed 5 cycles (8 min each). The maximum contraction achieved for this particle loading of 0.5 wt %, was of approximately 23% when the field strength was about 49 kA/m. The length change response is comparable to what has been reported for a similar magnetic LCE, whose maximum contractions were of 26% for much higher loadings of 1.64 vol% [9].

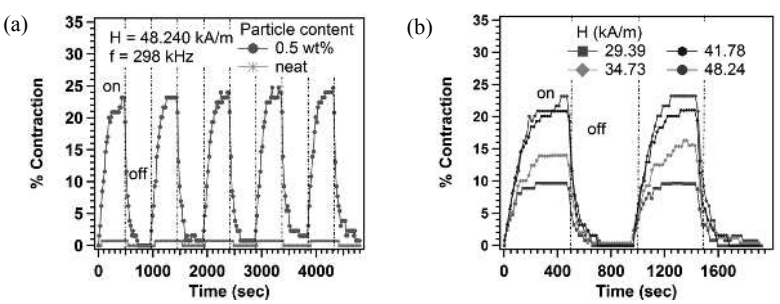

Figure 4. Magneto-mechanical behavior of the MLCE with 0.5 wt% particle loading subjected to five on/off cycles of an alternating magnetic field (a), and effect of magnetic field strengths during the first two on/off cycles (b).

Figure 4b shows the magneto-mechanical actuation behavior as a function of magnetic field strength, where the contraction increases with increasing field strength. The actuation mechanism as suggested in the literature is possibly due to heat dissipation by the magnetic nanoparticles which oscillate when subjected to magnetic fields, thus triggering the deformations in the LCE. The maximum contractions observed in Fig 4b show a linear dependency with field strength, which indicates that higher magnetic fields should be able to dissipate heat and induce larger deformations. A similar contraction magnitude would be observed if the elastomer temperature is increased from 25 to 40 °C as shown in Figure 2. Nevertheless, measurements of the temperature of the elastomers when subjected to magnetic fields are still required to demonstrate that deformations are due to a particle heat dissipation mechanism.

CONCLUSIONS

The inclusion of oleic acid-coated iron oxide nanoparticles yields homogeneous LCEs with particle loading-dependent liquid crystal phase transitions, with adjustable thermo-mechanical properties that can be tailored by changing the amount of particles embedded in the elastomeric matrix and with improved mechanical properties or increased stiffness. Also leads to LCEs that can be actuated remotely and that reveal reversible expansion/contractions in response to external magnetic fields by using lower amount of particles compared to what has been used before in the literature. These LCEs hold the promise for applications in actuation, sensing, or as smart active substrates, where dynamic changing physical conditions are required.

ACKNOWLEDGMENTS

This work was supported by the National Science Foundation under Grant No. DMR-0934115.

REFERENCES

1. R. Zentel, *Angew. Chem. Int. Ed. Engl. Adv. Mater.*, **28,** 1407 (1989).
2. F. J. Davis, *J. Mater. Chem.*, **3**, 551, (1993).
3. C. Ohm, M. Brehmer, and R. Zentel, *Adv. Mater.*, **22**, 3366 (2010).
4. C. Li, Y. Liu, C. Lo, and H. Jiang, *Soft Matter*, **7**, 7511 (2011).
5. L. Yang, K. Setyowati, A. Li, S. Gong, and J. Chen, *Adv. Mater.*, **20** 2271 (2008).
6. S. Courty, J. Mine, A. R. Tajbakhsh, and E. M. Terentjev, *Europhys. Lett.*, **64**, 654 (2003).
7. J. M. Haberl, A. Sánchez-Ferrer, A. M. Mihut, H. Dietsch, A. M. Hirt, and R. Mezzenga, *Adv. Mater.*, **25**, 1787 (2013); *Nanoscale*, **5**, 5539 (2013).
8. O. Riou, L. Zadoina, B. Lonetti, K. Soulantica, A.-F. Mingotaud, M. Respaud, B. Chaudret, and M. Mauzac, *Polymers,* **4**, 448 (2012).
9. A. Kaiser, M. Winkler, S. Krause, H. Finkelmann, and A. M. Schmidt, *J. Mater. Chem.*, **19**, 538 (2009).
10. J. Küpfer and H. Finkelmann, *Makromol. Chem. Rapid Commun.*, **12**, 717 (1991).
11. S. A. Ali, H. A. Al-Muallem, S. U. Rahman, and M. T. Saeed, *Corros. Sci*., **50**, 3070 (2008).
12. V. Domenici, V. V Laguta, and A. G. Belous, *J. Phys. Chem. C*, **114**, 10782 (2010).
13. F. Chen, A. Clough, B. M. Reinhard, M. W. Grinsta, N. Jiang, T. Koga, and O. K. C. Tsui, *Macromolecules*, **46**, 4663, (2013).
14. T. Hanemann and D. V. Szabó, *Materials,* **3,** 3468 (2010).
15. Y. Ji, J. E. Marshall, and E. M. Terentjev, *Polymers*, **4**, 316 (2012).
16. S.Y. Fu, X.Q. Feng, B. Lauke, and Y.W. Mai, *Compos. Part B Eng.*, **39**, 933 (2008).

Mater. Res. Soc. Symp. Proc. Vol. 1718 © 2015 Materials Research Society
DOI: 10.1557/opl.2015.492

Anisotropic Composites of Desaminotyrosine and Desaminotyrosyl Tyrosine Functionalized Gelatin and Bioactive Glass Microparticles

Konstanze K. Julich-Gruner[1], Andreas Lendlein[1], Aldo R. Boccaccini[2], and Axel T. Neffe[1]

[1] Institute of Biomaterial Research and Berlin-Brandenburg Centre for Regenerative Therapies, Helmholtz-Zentrum Geesthacht, Kantstrasse 55, 14513 Teltow, Germany
[2]Institute of Biomaterials, University of Erlangen-Nuremberg, Cauerstraße 6, 91058 Erlangen, Germany

ABSTRACT

Functionalization of gelatin with desaminotyrosine (DAT) and desamino tyrosyl tyrosine (DATT) has been demonstrated to allow network formation based on non-covalent interactions of the aromatic moieties. Based on the observation that the DAT(T) groups furthermore could interact with hydroxyapatite fillers, here it was investigated whether such interactions of DAT(T) could also be employed to stabilize composites formed by functionalized gelatins and bioactive glass (BG) particles. Because of sedimentation of the BG microparticles during the gelification, anisotropic composites with two distinct layers were formed. The characterization of mechanical properties by tensile tests and rheology showed that all composites of non-functionalized and DAT(T) functionalized gelatins with BG microparticles showed an increased Young's modulus (E) up to 3 MPa, an increased storage modulus (G') up to 100 kPa, increased tensile strength (σ_{max}) up to 3.4 MPa, and increased loss modulus (G'') compared to the pure matrices. As the observed effects were more pronounced in the DAT(T) functionalized gelatins compared to non-functionalized gelatins, and a much increased thermal stability of these composites was found, it is likely that there are binding interactions between the aromatic moieties and the BG microparticles. This effect open opportunities for the further development of this type of gelatin-based composites for bone regeneration applications.

INTRODUCTION

Natural materials having to provide strength and elasticity, such as teeth, bone, or seashells, are often composites of a biopolymeric matrix and an inorganic filler [1]. By changing aspect ratio, relative concentration of filler and matrix, or by enabling binding interaction between the two, the resulting mechanical properties of the composites can be tailored [2]. In this context, it could be shown that introduction of desaminotyrosine (DAT) or desaminotyrosyl tyrosine (DATT) on the backbone of gelatin not only enabled the formation of physical networks and allowed tailoring of triple helicalization by drying procedures[3], but also that these moieties furthermore led to an increase of the Young's modulus (from 200 kPa up to 2 MPa), tensile strength (from 57 kPa up to 1.1 MPa), and the thermal stability (from 40 to 85 °C) in hydroxyl-apatite composites compared to the pure matrices without affecting the elongation at break [4]. Through comparison with composites of unfunctionalized gelatins by spectroscopical methods and mechanical tests, this behavior could be rationalized by stabilizing bonds between the phenol moieties and hydroxyapatite. Hydroxyapatite composites have been shown to display increased biocompatibility and support of bone growth compared to pure polymers *in vitro* and *in vivo* and are therefore of interest for bone healing applications [5]. On the other hand bioactive glasses

(BGs) have been attracting increasing attention for bone regeneration applications, as exchange reactions on the surface of BGs result *in vitro* and *in vivo* in the formation of a surface hydroxyapatite layer leading to enhanced attachment and growth of osteoblasts [6, 7]. Silicate BGs are a family of glasses based on the SiO_2-P_2O_5-CaO-Na_2O system which can be also incorporated with other metallic oxides for enhanced biological activity [8]. The most commonly applied BG is the composition 45S5 BG (in wt%: 45 SiO_2, 24.5 CaO, 24.5 Na_2O and 6 P_2O_5), which was first reported in 1971 [9] and has been considered for numerous medical applications [7]. In the present study it was investigated, if the DAT(T) functionalized matrices also engage in binding interactions to 45S5 BG microparticles (µBG) as fillers. By using µBG, partial sedimentation during gelation results in asymmetric composites films, which may be useful for applications such as materials inducing osteochondral defect repair by mediating simultaneously contact to hard (high µBG content) and soft tissues (low µBG content) [10]. In the following, the formation of the composites with a nominal µBG content of 10, 20 or 50 wt.-% and the characterization of their thermomechanical properties are reported. Due to the layered structure, the interpretation of mechanical properties should be evaluated as preliminary, as the individual parts containing more or less µBG likely differ in their properties. The composites will be referred to as matrix-XX, with XX giving the nominal wt.-% content µBG.

EXPERIMENTAL DETAILS

Materials: All chemicals were received from Sigma-Aldrich (Munich, Germany). Gelatin (porcine skin, Type A, 200 Bloom) was functionalized with desaminotyrosin or desamino tyrosyl tyrosin as described before [3]. In short, DAT or DATT were activated by reaction with 1-ethyl-3-dimethylaminopropyl carbodiimide and *N*-hydroxysuccinimide in DMSO at 37 °C, added to a gelatin solution in DMSO, and stirred for 5 h. Precipitation in ethanol, washing with ethanol and acetone, and drying under vacuum gave the functionalized products. Melt-derived µBG of composition 45S5 BG [9] and mean particle size < 7 µm were used.
Composite Formation: A dispersion of 120, 240, or 600 mg µBG in 20 ml water was sonicated (Bandelin Sonopuls HD2070, Berlin, Germany) for 1 h, and mixed with a solution of 1.2 g gelatin or Gel-DAT(T) prepared in 20 mL of water at 40 °C, cooled to r.t., and the mixture was stirred for 1-2 min. Drying at r.t. and normal pressure gave the composites.
Electron Microscopy was conducted with a SUPRA 40 VP electron microscope with a Schottky emitter at an acceleration voltage of 3 kV (Carl Zeiss NTS GmbH, Oberkochen, Germany).
Thermogravimetric Analysis (TGA) was carried on a thermo microbalance (Netzsch GmbH, Selb, Germany TG 209C) under a nitrogen atmosphere within the temperature range of 25 to 850 °C at a heating rate of 10 $K \cdot min^{-1}$.
Temperature Modulated Differential Scanning Calorimetry (TM-DSC) was measured on a Phönix DSC 204 F1 (Netzsch GmbH, Selb, Germany) apparatus. The gelatin samples were hermetically sealed in an aluminium pan. Two consecutive heating runs from -20 to 150 °C in the first heating run and up to 250 °C in the second heating run were performed with a modulated heating rate with a period of 60 s, amplitude of 0.5 °C, and an underlying heating rate of 5 °C · min^{-1}. Between heating runs, the samples were rapidly cooled (10 °C·min^{-1}).
Swelling (*Q*) and Water Uptake (*H*): Samples prepared through drying at r.t. at normal pressure (see above) were further dried in vacuum to remove water to the highest possible extent without allowing chain re-organization. The samples were weighed before immersing them in distilled water. Samples were kept in temperature controlled water baths at 22 or 37 °C for 24 h. After

removal of excess water with a pipette, mass and volume of five replicates were determined. Water uptake and swelling were calculated according to equations 1 and 2:

$$H = [(m_{sw} - m_{dry}) \cdot m_{dry}^{-1}] \quad \text{eq. 1}$$

$$Q = 1 + \rho_{comp} \cdot [(m_{sw} \cdot m_{dry}^{-1} \cdot \rho_{H2O}^{-1}) - \rho_{H2O}^{-1}] \quad \text{eq. 2}$$

where m_{sw} refers to net weight of the respective hydrogel in the swollen state, m_{dry} is the vacuum dried weight, ρ_{comp} is the density of the relevant composite determined via pycnometry and ρ_{H2O} is the density of distilled water, assumed to be 1.00 g·cm^{-3} (the difference between room temperature and 37 °C is ~0.004 g·cm^{-3}).

Tensile tests were conducted on dog-bone-shaped (20 mm in length and 2 mm in width) samples punched out of swollen hydrogels. Tests were performed on five replicates at room temperature at a strain velocity of 1 mm·min^{-1}, and maximum applied stress of 1.25 N. Data recording started at a force threshold of 0.01 N on a universal tensile testing machine (Zwick Z 2.5, Zwick-Roell, Ulm, Germany) with a load cell of 50 N.

Wide-Angle X-ray Scattering (WAXS) investigation was performed on a Bruker D8 Discover (Bruker AXS, Karlsruhe, Germany). The X-ray generator was operated at a voltage of 40 kV and a current of 40 mA. A copper anode and a graphite monochromator produced Cu K_α radiation with a wavelength $\lambda = 0.154$ nm. WAXS images were collected from dried gelatin composite films in transmission.

Rheological measurements were performed with a plate–plate rheometer (Haake MARS II Thermo Fisher) with RheoWin software using a Peltier element of 20 mm diameter. All dynamic measurements were performed on rehydrated gelatin composites in the linear viscosity region applying a constant normal force of 1 Pa. All samples were previously swollen in water at equilibrium and were covered to prevent evaporation of the solvent during measurement. The temperature dependence of the storage modulus was determined from the oscillatory shear stress with a temperature scan from 15 to 70 °C with a heating rate of 1.8 K·min^{-1} at a constant frequency (1 Hz).

RESULTS AND DISCUSSION

The composites were prepared by mixing a 6 wt.-% aqueous solution of gelatin or Gel-DAT(T) at room temperature with a dispersion of µBG in the same amount of water, and letting the system to gelate and dry. Drying was completed within 96 h. During the time of gelation, the µBG partially sedimented to give anisotropic films as depicted exemplarily in Fig. 1. In case of the formerly investigated hydroxy apatite composites, a homogenous distribution of the filler in the matrix was achieved [4]. The further characterization of the anisotropic, layered composites investigated here has to be evaluated taking into account that the two distinct layers probably display quite different properties, and that the data presented have contributions from each of these layers. This will be pointed out in the discussion of the individual data when relevant. So far, it was not possible to separate the two layers by cutting. The actual µBG content in the samples was determined by thermogravimetric analysis (see Table 1). The final µBG content increased with amount of µBG added during composite formation, and the nominal and actual values were in reasonable agreement, especially for Gel-DAT and all 50 wt.-% composites. Table 1 summarizes the thermal transitions, water uptake and swelling, as well as the mechanical properties of the samples determined in tensile tests. Temperature modulated DSC of dried samples allowed the determination of the glass transition temperature T_g and the melting temperature T_m, with the melting transition corresponding to the melting of triple helices. The T_g

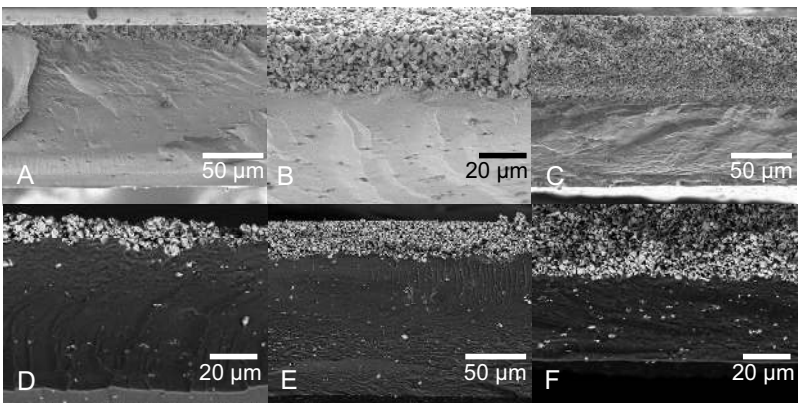

Figure 1. Scanning electron microscopy of Gel-DAT-10 (A), -20 (B), and -50 (C) as well as Gel-DATT-10 (D), -20 (E), and -50 (F) composite films showing the formation of asymmetrical layered structures.

values of the composites were drastically reduced (by 30-70 °C) compared to the pure matrices. The decreasing T_g with increasing µBG content suggests a higher chain mobility in the composites than in the pure matrices. At the same time, composite formation led to an increase of T_m indicating a stabilization of triple helices. It is well possible that the thermal transitions in the two layers are different and average values were recorded. The stabilization of triple helices could also be shown in WAXS spectra (Fig. 2A), with the increasing peak at 32° indicating an increasing amount of single helices with increasing µBG content. This stabilization of helices could be either due to the µBG, or due to released ions interacting with the protein chains. It has been shown earlier that the metal ion content of protein-based biomaterials has a strong influence on chain organization and mechanical properties [11, 12]. A further explanation of the high single helical content may be associated with the lowering of T_g. Helicalization in gelatin-based systems is thermodynamically favored, but kinetically hindered. In the investigated systems, the kinetic hindering might be reduced, allowing for faster helicalization. Again, the WAXS data are averaged over the two phases and might differ in the individual layers. Water uptake and swelling were generally lower in the anisotropic composites than in the pure matrices, however, no linear trend for relating µBG content and H or Q was found. H and Q depend on the content of swellable component as well as the number of netpoints, which do not linearly change with µBG content. Probably, the layer with higher µBG content shows lower swelling and water uptake than the layer with lower filler content. Furthermore, H and Q were lower in the functionalized gelatin composites than in the gelatin composites. The gelatin composites as well as Gel-DAT samples dissolved in water at 37 °C over time, therefore H and Q were determined at 25 °C for these samples. In tensile tests, it could be shown that the µBG containing composites have higher Young's moduli and tensile strength than the pure matrices. Interestingly, the nominally 10 wt-% µBG containing composites showed the highest E and σ_{max} values. While the composite formation procedure gave asymmetric films by design, the inhomogeneity might lead to some artifacts in the tensile tests of higher µBG content, which also show stronger asymmetry. Likely, the layer with higher µBG content contributes to E, σ_{max} and ε_b more strongly than the layer with lower µBG content. The Young's moduli of the composites in the lower MPa range